The Influence of Solvation and Finite Temperatures on the Wittig Reaction: A Theoretical Study

Michael Seth, Hans Martin Senn,† and Tom Ziegler*

Department of Chemistry, University of Calgary, 2500 University Drive NW, Calgary, AB T2N-1N4, Canada

Received: October 13, 2004; In Final Form: March 11, 2005

The effects of the solvent and finite temperature (entropy) on the Wittig reaction are studied by using density functional theory in combination with molecular dynamics and a continuum solvation model. Standard gas-phase zero-temperature calculations are found to give similar results to previous studies. Gas-phase dynamics simulations allow the free energy profile of the reaction to be calculated through thermodynamic integration. The free energy profile is found to have a significant entropic barrier to the addition step of the reaction where only a small barrier was present in the potential energy curve. The introduction of the solvent dimethyl sulfoxide causes a change in the structure of the intermediate from the oxaphosphetane structure to the dipolar betaine structure. The overall reaction energy is changed only slightly. When the effects of both entropy and the solvent are included a significant entropic barrier to the addition reaction is obtained and the predicted intermediate again has the betaine structure.

1. Introduction

Over the past few decades quantum mechanical calculations have provided considerable insight into the mechanisms of chemical reactions. Through careful examination of important regions of the potential energy hypersurface calculated by theoretical methods, proposed transition states and intermediates can be evaluated and compared. Ultimately, such a comparison can help to support or further question proposed mechanisms.

A case in point is the Wittig reaction. Developed by Wittig and co-workers,[1,2] the Wittig reaction involves the addition of an aldehyde or ketone to a phosphorus ylide to form an alkene and a phosphine oxide. It has been a useful part of the armory available to the synthetic organic chemist for a number of years.[3,4] The starting materials are typically an aldehyde or ketone with the desired structure and an appropriate alkyl halide. The alkyl halide is reacted with a trialkyl or triaryl phosphine to produce a phosphonium salt. This is then deprotonated by a strong base to yield the ylide. The reaction has the extremely useful feature that it forms a new carbon−carbon double bond joining two molecules. Since an alkene is formed the area can readily be further functionalized. A wide variety of aldehydes and ketones and alkyl halides can be successfully reacted through the Wittig reaction with good control over the product stereochemistry. Some useful variations on the Wittig reaction exist where phosphonates and phosphine oxides rather than phospines are used as one of the starting materials (Wadsworth−Evans and Horner−Wittig reactions).[4]

Proposed mechanisms for the Wittig reaction suggest that it is a two-step process: an initial addition reaction to form an intermediate followed by an elimination reaction to form the products (Chart 1). Two possible intermediate structures have been proposed. The first is a dipolar betaine with the first C−C bond of the product alkene formed and formal negative and positive charges on the O and P atoms, respectively. The other proposed intermediate is the product of a concerted or nearly

CHART 1

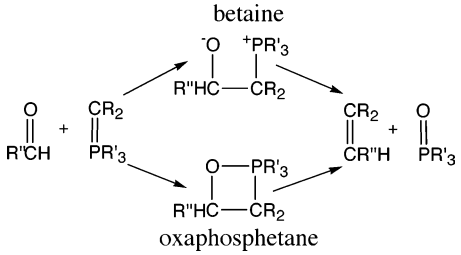

concerted cycloaddition of the ylide and carbonyl groups to form a four-membered oxaphosphetane ring. Considerable effort has gone into identifying the intermediates present but no definitive answer has been reached as yet. Early work pointed toward the betaine intermediate but experimental studies have favored the oxaphosphetane intermediate.[5−9]

The first ab initio study of the Wittig reaction was a restricted Hartree−Fock (RHF) study carried out by Höller and Lischka.[10] In this work the reaction $PH_3CH_2 + CH_2O \rightarrow PH_3O + C_2H_4$ was examined. A minimum in the potential energy surface corresponding to the oxaphosphetane was identified but no evidence of a betaine intermediate was observed. The initial addition reaction was calculated to have a very low reaction barrier (≈5 kcal/mol) and to be exothermic by about 34 kcal/mol. Starting from the oxaphosphetane, the dissociation reaction was determined to have a significant barrier (≈24 kcal/mol) and to be exothermic by about 14 kcal/mol giving an overall reaction energy of −45 to −50 kcal/mol. The arrangement of atoms about the five-coordinate P center was found to change from oxygen axial and carbon equatorial in a trigonal bipyramid to oxygen equatorial and carbon axial also in a bipyramid during the course of the reaction. However, neither was found to be the clear-cut better candidate for the coordination geometry of the intermediate.

Subsequent calculations have expanded upon and refined the work of Höller and Lischka while still supporting their qualitative conclusions. More accurate calculations considering the

† Present address: Max-Planck-Institut für Kohlenforschung, D-45470 Mülheim an der Ruhr, Germany.

10.1021/jp045318i CCC: $30.25
Published on Web 05/19/2005

same reactants gave largely the same results[11−13] and found the oxaphosphetane intermediate with the O atom axial to be lower in energy. Semiempirical calculations on larger molecules also predicted a qualitatively similar mechanism.[14−16] Yamataka and Nagase performed B3-LYP calculations on several more realistic reactant systems such as $Ph_3P{=}CHPh + PhCHO$.[17] Unlike the previous ab initio studies, this work was able to examine the stereoselectivity of the reaction. Although the addition of phenyl rings to the ylide and the carbonyl group led to modifications in the structures of the addition transition states, the overall reaction scheme of oxaphosphetane formed with very low barrier followed by higher barrier to products was again obtained. Lu and co-workers considered the reaction of $X_3P{=}CH_2$ and $H_2C{=}O$ where X = F, H, Me, and Ph.[18] Their results were similar to those already discussed although the case where X = F was found to be somewhat different from the other three. Perhaps more importantly for the purposes of the present study, this work found that the system where X = Me is a very good model of the real system where X = Ph.

Whenever theoretical calculations on molecular species are performed a number of approximations are employed to keep the calculations tractable. The studies involving the Wittig reaction are of course no exception to this. For the most part, the approximations made in the studies described in the previous paragraph are reasonable and are likely to introduce small errors of known magnitude. One of the approximations, the use of a model of the true system, was eliminated completely in the work of Yamataka and Nagase.[17] Two of the approximations, however, namely the neglect of the solvent and the neglect of finite temperature effects, could conceivably lead to more significant errors being introduced.

Wittig reactions are almost always carried out in solution with the synthetic chemist having the choice of a number of solvents depending on the exact reagents and desired products. One possible structure for the intermediate in a Wittig reaction, the betaine, is significantly more polar than either the reactant or the products and would be expected to be favored by the inclusion of solvent effects.

The neglect of entropy by considering simple energy differences and reaction enthalpies rather than free energies could be a serious approximation since it is free energies that govern reaction rates and equilibrium constants. Free energy barriers and free energies of reaction might be expected to give a more realistic view of how the reaction actually proceeds.

With enough computer power at hand, it is now possible to eliminate or at least minimize the effect of most approximations (though probably not all at the same time) when studying a chemical reaction involving small to medium-sized molecules. Some allowance for solvent and finite temperature effects certainly can be made. It was the goal of the work described in this paper to uncover just what influence the inclusion of solvation and entropy will have on theoretical predictions concerning the Wittig reaction.

Given the computational resources available, it was not possible to use a completely realistic model for the reactants in a Wittig reaction while still including all of the other desired properties in the calculations. It was decided to model the ylide as $Me_3P{=}CH_2$ and to take the carbonyl group-containing molecule to be CH_3CHO. The work of Lu and co-workers[18] suggests that studies of the smaller system should provide results directly applicable to the more commonly used $Ph_3P{=}CH_2$ reagent. No stereodifferentiation is possible with these reagents and the present work cannot say anything about this aspect of the Wittig reaction.

The direct participation of a solvent molecule is not generally invoked in proposed mechanisms of the Wittig reaction. A continuum approach to solvation[19−24] then should be capable of introducing solvent effects into theoretical calculations of this reaction. In any case, the explicit inclusion of a number of solvent molecules would quickly make the calculation impossible due to the large number of atoms involved. A number of continuum models have been proposed in the literature. The particular method chosen was the conductor-like screening model (COSMO)[25,26] as implemented by Senn and co-workers.[27] The solvent was chosen to be dimethyl sulfoxide (DMSO). DMSO has a dielectric constant of 46.7 and as such is one of the more polar solvents used in Wittig reactions. Any solvent effects observed should thus be regarded as being on the high end of the range.

Finite temperature and entropy effects can be included into a quantum mechanical calculation in different ways. The approach of molecular dynamics in combination with pointwise thermodynamic integration[28] was chosen. This method was used in preference to the frequency analysis approach, which is more often used in quantum chemical calculations because the free energy at many points along the reaction coordinate was required. The harmonic approximation implicit in most frequency analyses[29] is likely to break down in regions where two molecules are in close proximity but only weakly interacting and this method was therefore deemed inappropriate for deriving the free energy profile of addition and elimination reactions such as those investigated here.

2. Computational Details

The electronic structure in the present calculations was described by using density functional theory (DFT). The functional used is the combination of the exchange functional described by Becke[30] and the correlation functional described by Perdew[31] in combination with the parametrization of the electron gas correlation energy of Perdew and Wang.[32]

The nuclear dynamics performed on an ab initio potential energy surface utilized the Car−Parrinello approach[33] with the projector-augmented wave (PAW) method of Blöchl.[34,35] The [He] core of the C and O atoms was kept frozen as was the [Ne] core of the P atom. 2s2p1d sets of projectors were used in combination with the heavier atoms while a 2s1p set was used for the hydrogen atoms. The plane-wave basis set was defined through an energy cutoff of 30 Ry (15 au) and a density cutoff of 60 Ry (30 au) in a face-centered cubic unit cell of side 13.01 Å. The time evolution of the system was integrated with a time step of 5 au (0.12 fs). The masses of the nuclei were taken to be 2.014, 12.00, 15.995, and 30.94 amu for H, C, O, and P, respectively, and the fictitious mass of the wave function was chosen to be 250 au. To sample the NVT (canonical) ensemble rather than the NVE (microcanonical) ensemble the stochastic thermostat of Andersen[36] was applied to the nuclear motion. A temperature of 300 K was maintained by reassigning the velocities of three randomly chosen atoms every 12 time steps. The temperature of the wave function was moderated by applying a constant friction of $0.001/\Delta t$. All simulations were carried out with the translation of the center of mass and rotation of the total system removed.

Energy differences at 0 K will be denoted by ΔE while the free energy differences obtained at 300 K will be denoted ΔA. Helmholtz free energies are obtained here rather than Gibbs free energies (ΔG) as the volume of the system rather than the pressure is kept constant.

Since the orbitals are described in terms of a plane-wave basis set, the calculation will actually describe a three-dimensional

periodic system of molecules. To remove the interaction between different images and accurately simulate an isolated reaction an electrostatic decoupling scheme was applied.[37]

The details of the implementation of COSMO[25,26] applied in the present study can be found in ref 27. In addition to the dielectric constant of the solvent COSMO calculations require the input of a few other parameters. The sphere radii for H, C, O, and P were chosen to be 2.2, 3.6, 3.2, and 4.0 au, respectively, the fictitious mass of the charges was chosen to be 12.0 au, their motion was damped by a friction of $0.001/\Delta t$, and their motion was oversampled by a factor of 30 with respect to the other degrees of freedom. Sixty surface segments were used for each atomic sphere. The nonelectrostatic parameters were $(4.569 \times 10^{-4})E_h$ (β) and $(1.1661 \times 10^{-6})E_h/a_0$ (γ).

All calculations were performed with a modified version of the Car−Parrinello Projector Augmented Wave program, PAW of Blöchl.[34,37,38]

The potential energy curves were obtained by first heating the system up, then cooling it to 0 K at a number of values of the reaction coordinate. In the reactants and products regions of the reaction curve the potential energy surface is very flat with a number of local minima corresponding to different relative orientations of the reactant and product molecules for any given value of the reaction coordinate. Optimizations in this region often fell into the lowest of these minima but about as often did not leading to a very "kinky" potential energy curve. At values of the reaction coordinate where the optimization did not fall into the lowest of the minima the optimization was repeated from a new starting point until a more reasonable energy was obtained.

ΔA was calculated following the procedures outlined in refs 28 and 39. The reaction coordinate of the addition step (R_1) was taken to be the distance between the center of mass of the P and C of the ylide and the center of mass of the sp^2 C and O of the ethanal molecule. For the dissociation reaction, it was taken to be the distance between the center of mass of the two carbon atoms from the propene double bond and the center of mass of the phosphorus and oxygen atoms (R_2). Starting geometries were obtained by minimizing the energy of the system at 0 K in the region of the potential energy hypersurface corresponding to the oxaphosphetane. Once a starting geometry was found, the geometrical parameter corresponding to the reaction coordinate of interest was constrained and the molecule was heated to 300 K. The system was allowed to propagate at 300 K at this value of the reaction coordinate for 6 ps to ensure equilibration.

The initial positions and velocities at several values of the reaction coordinate required for point-wise thermodynamic integration were obtained by starting from the system equilibrated at one value of the reaction coordinate and varying that coordinate quite slowly (about 2 Å ps^{-1}) until the important range of values of the coordinate of interest was covered. Enough points (20−40 depending on the shape of the free energy profile) along the reaction coordinate were taken to ensure that the numerical integration performed later was acceptably accurate (numerical error <0.5 kcal/mol). At each of these values of the reaction coordinate a 3.6 ps trajectory was calculated. The first 1.8 ps of each was discarded to ensure equilibration at that value of the reaction coordinate and the remainder used to obtain the ensemble average of the constraint force ($\langle F_\lambda \rangle_{NVT}$) at the value λ of the reaction coordinate. These average forces at each value of the reaction coordinate were integrated by Simpson's method to obtain the desired free energy differences from one point on the reaction curve to another, ΔA.

TABLE 1: Energy Changes and Geometrical Parameters of the Wittig Reaction in the Gas Phase at 0 K[a]

	ΔE	R_{1or2}	R_{PC}	R_{CO}	R_{CC}	R_{PO}	ϕ_{PCCO}
reactants	0.0		1.69	1.22			
TS 1	1.6	2.78	1.77	1.30	1.85	3.22	−41
intermediates	−18.1	1.79/1.72	1.86	1.43	1.54	1.87	−8
TS 2	0.8	2.18	2.45	1.75	1.44	1.61	0
products	−44.4				1.34	1.50	

[a] Energies in kcal/mol. Distances in Å. Angles in degrees.

Owing to the constraints upon translation and rotation of the whole system applied in all calculations, some of the reaction entropy changes ΔS are not included. The missed entropy changes were added back in by applying the correction formula given in ref 39.

The addition reaction in the gas phase provided a technical difficulty in the present calculations. At two values of the reaction coordinate ($R_1 = 2.51$ and 2.65 Å) of the cyclization reaction in the gas phase at 300 K the oxygen atom would, after a fairly short period of time, abstract a hydrogen from one of the methyl groups attached to the phosphorus. This alternative reaction path is not of interest for two reasons. First, the hydrogen abstraction is only able to take place because the more favorable (larger energy gradient along this direction) reaction leading to the oxygen and phosphorus forming a bond is prevented by the constraint. Second, ylides employed in Wittig reactions usually have phenyl groups as the nonparticipating phosphorus ligands. Phenyl groups have no α-hydrogens to be transferred to the oxygen atom.

It was therefore undesirable for the H-transfer reaction to take place. To avoid this, an additional short-range repulsive potential between the oxygen atom and the methyl hydrogens was included in the simulations at $R_1 = 2.51$ and 2.65 Å. The potential was exponential in form and had a value of 23 000 kcal/mol when the O and H atoms were separated by the sum of their covalent radii (1.05 Å) and decayed by a factor of 10 000 for each additional 1.05 Å of separation. A test calculation at a nearby value of R_1 found that the addition of such repulsive potentials had little effect on the calculated value of $\langle F \rangle$.

3. Results and Discussion

3.1. The Reaction at 0 K in the Gas Phase. The first case that will be considered is that where solvent and finite temperature effects are neglected. This is the same level of approximation as that applied in all other studies of the Wittig reaction and will constitute our baseline from which the influence of solvent and temperature will be judged.

For each of the important points along the reaction coordinate, namely reactants, the transition state of the addition reaction, the intermediate, the transition state of the dissociation reaction, and products, their energy relative to reactants (ΔE), the value of the reaction coordinate (R_1 or R_2) and several important geometrical parameters are listed in Table 1. The particular parameters chosen are the distances between neighboring atoms of the four-membered ring of the oxaphosphetane (R_{PC}, R_{CO}, R_{CC}, and R_{PO}) and the dihedral angle of the ring with the atoms in the sequence P−C−C−O (ϕ_{PCCO}). The structures of the two transition states and the intermediate are illustrated in Figure 1. The potential energy curves of both steps of the reaction are shown on one graph in Figure 2. They are arranged such that they meet in the central minimum corresponding to the reaction intermediate. On the left-hand side of the figure, the reaction

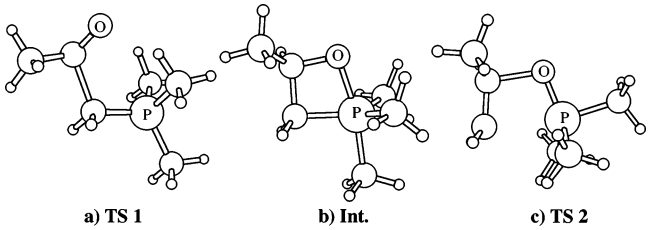

Figure 1. Structures of the transitions states and the intermediate of the Wittig reaction in the gas phase at 0 K. The intermediate has the oxaphosphetane structure. All unlabeled atoms are either C or H.

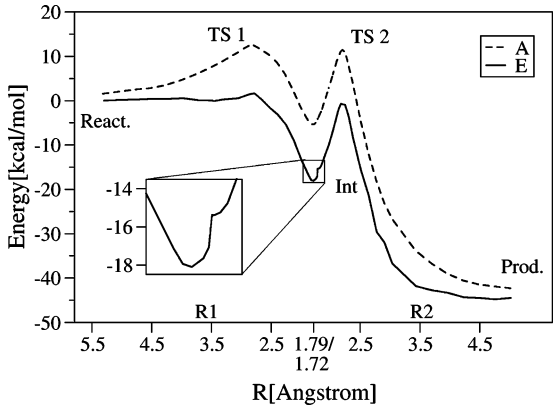

Figure 2. Helmholtz free energy and potential energy as a function of reaction coordinate of the Wittig reaction in the gas phase.

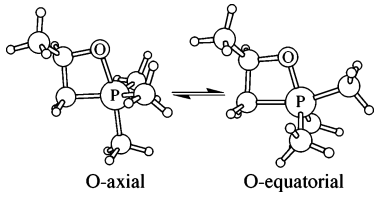

Figure 3. Possible structures of the oxaphosphetane intermediate related by a pseudorotation. All unlabeled atoms are either C or H.

coordinate is R_1, which varies from 5.29 to 1.79 Å at the intermediate. The right-hand part of the figure corresponds to the second reaction coordinate, which varies from 1.71 Å at the intermediate to 5.0 Å at the rightmost end.

As would be expected, the potential energy curve of the reaction in the gas phase is very similar to that described by previous calculations. As the reactants approach each other they pass over a small barrier 0.5 kcal/mol in height before reaching a very shallow minimum 0.1 kcal/mol below the separated reactants. This minimum has been observed previously[10,13,17,18] and is usually described as a van der Waals complex. The transition state of the association reaction is at a value of R_1 of about 2.8 and is also very low in energy ($\Delta E^{\ddagger}_{add} = 1.6$ kcal/mol). In the transition state the C−C bond is nearly fully formed ($R_{CC} = 1.85$ Å) and the C−O is still elongated ($R_{CO} = 3.22$ Å, Figure 1a. The reaction is clearly proceeding to a oxaphosphetane, which is indeed the structure of the intermediate (Figure 1b). The intermediate is formed exothermically ($\Delta E_{int} = -18.1$ kcal/mol) and has the O atom in an axial position with respect to the phosphorus.

The molecule is found to undergo a pseudorotation before proceeding to products with the O atom in an equatorial position (Figure 3). Since the local minimum in the potential energy curve corresponding to the O-equatorial isomer is close in energy and value of the reaction coordinate R_2 to the O-axial isomer ($R_2 = 1.80$ for the O-equatorial minimum and 1.72 for the O-axial structure) it is difficult to see in Figure 2. This part of the potential energy curve was enlarged (inset, Figure 2) to make the situation clearer. As was found by Lu and co-workers,[18] the O-equatorial isomer is slightly higher (2.7 kcal/mol) in energy and the reaction O-equatorial → O-axial proceeds with a very low barrier (<0.1 kcal/mol). The barrier of the pseudorotation is difficult to estimate from the current calculations as the reaction coordinate chosen to describe the transformation from the intermediate to products is not particularly suitable for describing the pseudorotation.

TABLE 2: Free Energy Changes and Geometrical Parameters of the Wittig Reaction in the Gas Phase at 300 K[a]

	ΔA	R_{1or2}	R_{PC}	R_{CO}	R_{CC}	R_{PO}	ϕ_{PCCO}
reactants	0.0		1.69	1.22			
TS 1	12.7	2.78	1.75	1.28	2.09	3.14	−56
intermediates	−5.8	1.77/1.73	1.88	1.44	1.54	1.85	−2
TS 2	11.1	2.21	2.47	1.81	1.43	1.60	−1
products	−43.4				1.34	1.51	

[a] Energies in kcal/mol. Distances in Å. Angles in degrees.

The dissociation reaction has a barrier that is significant with respect to the intermediate (about 20 kcal/mol). The energy of this transition state is in fact very similar to that of the reactants ($\Delta E^{\ddagger}_{diss} = 0.8$ kcal/mol).

The dissociation reaction is exothermic leading to an overall reaction energy of −44 kcal/mol. Both the P−C and C−O bonds are significantly elongated in the transition state with the P−C bond showing the greater increase, but the four atoms still lie in a plane (Figure 1c and Table 1). Not long after the transition state, but still in a region of the potential energy surface where there is significant repulsion between the two product molecules, the propylene molecule undergoes a rotation such that the newly formed C−C double bond is perpendicular to the P−O bond. This motion is probably caused by the molecules attempting to minimize steric repulsion.

All of the results described in this section are very much in line with previous calculations.

3.2. The Reaction at 300 K and in the Gas Phase. The first modification that will be introduced into the calculations is the addition of finite temperature or entropy effects and the consideration of free energies of reaction ΔA rather than changes in potential energy ΔE. The free energy changes of the reaction ΔA and relevant geometric parameters are listed in Table 2. With the exception of the reaction coordinate, all of the geometric parameters are averages over the final 1.8 ps of the relevant trajectory. The free energy curves of the addition and dissociation reactions are given in Figure 2. Ensemble average forces were obtained for 28 values of R_1 coordinate between 1.7 and 5.3 Å for the addition reaction and a further 38 values of R_2 between 1.7 and 5.3 Å were calculated for the dissociation reaction. More points were included in the dissociation reaction in an attempt to characterize the region of the free energy profile where pseudorotation about the P atom could take place most readily.

It should be noted that the free energy is not zero at the largest value of R_1 (reactants) but rather is about 1.5 kcal/mol. This free energy results from the loss of entropy caused by constraining the two reactant molecules to be a relatively short distance apart and is calculated by using the formula from ref 39. The zero-point in free energy is taken at the point where $R_1 = \infty$.

The most obvious difference between the potential and free energy curves is associated with the transition state of the addition reaction. The barrier in the potential energy curve is very low, less than 2 kcal/mol. In contrast, the free energy curve has a significant barrier of about 12.5 kcal/mol. The first step

in the Wittig reaction is therefore predicted to have an almost purely entropic barrier. This is similar to the reaction of dichlorocarbene and ethene studied previously.[39] The barrier is the result of the loss of rotational entropy as the two molecules approach one another and the C−C bond is formed. The location of the transition state in the free energy curve is at almost the same value of R_1 as that of the potential energy curve. There is no sign in the free energy curve of the shallow minimum corresponding to a weakly bound complex found in the internal energy curve. It seems that such a shallow minimum will have no influence on the reaction once the reactants are heated to 300 K. The average P−C and C−O bond lengths are very similar to the equivalent bond lengths at the transition state on the internal energy surface (Table 2). In contrast, the average lengths of the newly forming P−O and C−C bonds are significantly different. The PO and CC bonds are clearly still rather floppy at this point of the reaction. The standard deviations of R_{PO} and R_{CC} over the course of the simulation at $R_1 = 2.78$ Å are 0.13 and 0.22 Å, respectively, while those of R_{PC} and R_{CO} are more similar to what might be expected for a stable bond at 0.04 and 0.03 Å. In any case, the qualitative structure of the transition state is still similar to that found at 0 K. The C−C bond is more fully formed than the P−O bond, which is still significantly stretched.

As would be expected, the cyclization reaction is less exergonic than it is exothermic. It still has a negative ΔA_{int} of about −6 kcal/mol. The structure of the intermediate itself is still an oxaphosphetane. The average values of the bond lengths in Table 2 are very similar to those of the intermediate at 0 K shown in Figure 1b and they perform vibrations of relatively small amplitude and have standard deviations of less than 0.05 Å.

Since the betaine would be more floppy than the oxaphosphetane, it should be entropically favored. Clearly, it is not favored enough by entropy at 300 K in the gas phase to overcome the more advantageous bonding of the oxaphosphetane.

The shape of the free energy curve of the dissociation reaction is similar to that of the potential energy curve of the same reaction in that it has a significant maximum and then proceeds to energies well below the intermediate. The reaction free energy of this step is rather more negative than the change in potential energy (−37 kcal/mol as compared to −26 kcal/mol). This is due to the system gaining entropy as the products separate and are able to rotate individually again in the reverse of the situation encountered with the addition reaction.

The barrier height relative to the intermediate is largely unaffected and is only about 2 kcal/mol lower in the free energy curve. Thus, the majority of the rotational entropy of the two product molecules is gained after the transition state.

The average geometry at the second transition state in the free energy curve is very similar to the transition state geometry on the internal energy curve. All of the four bond lengths of the second transition state in Tables 1 and 2 are nearly identical. The breaking bonds are relatively flexible; R_{PC} and R_{CO} have standard deviations of 0.07 and 0.11 Å, respectively.

The overall free energy change of the whole reaction is similar to the total potential energy change. This is not so surprising since the number of molecules is the same at the beginning and end of the reaction and the overall entropy change would be expected to be relatively small.

Finally, the dynamics simulations allow us to follow the pseudorotation about the P atom as the dissociation reaction proceeds. At values of R_2 between 1.75 and 1.90 Å the two structures related by the pseudorotation are close in energy and can change into one another by traversing a very low barrier. Thus, at 300 K it would be expected that the molecule would jump back and forth between the two possibilities in simulations where R_2 is constrained to be somewhere in this range. From a visual inspection of some of the relevant trajectories, this does indeed seem to be the case. In the simulation carried out at the central minimum in the free energy profile ($R_2 = 1.73$ Å) the molecule remains in the O-axial isomer for the whole 3.6 ps of the simulation. It seems, therefore, that the O-equatorial isomer of this molecule is too high in energy to be present in significant quantities. This is what would be expected given the difference in energy of the two isomers of 2.7 kcal/mol, which is rather larger than kT (0.6 kcal/mol at 300 K). Once R_2 is constrained to take values larger than 1.75 Å the molecule begins to undergo the pseudorotation spending more and more time in the O-equatorial form until this is the only structure observed for values of R_2 greater than 1.92 Å. To put the analysis of the pseudorotation on a more quantitative footing, the O−P−C angles, where C is a carbon atom from any of the methyl groups, were evaluated over the trajectories of several simulations where $1.76 \text{ Å} \leq R_2 \leq 1.92$ Å. These angles provide a useful measure of whether the molecule is in the O-axial or the O-equatorial isomer as two of the angles are about 90° and one about 180° in the former case and two are about 120° one about 90° the latter. A geometry was taken to be O-axial if one angle was greater than 150° and to be O-equatorial otherwise. When $R_2 = 1.76$ Å the molecule is always O-axial by this measure. Starting with the simulation at $R_2 = 1.78$ Å the O-equatorial begins to appear (7% of the time) and is increasingly persistent until it is the only isomer observed when $R_2 = 1.92$ Å. Around $R_2 = 1.83$ Å the molecule can undergo the pseudorotation very easily and both isomers are observed about equally often.

In terms of the free energy profile, no minimum or even significant shoulder appears in the region where the pseudorotation occurs. It seems that the minimum corresponding to the O-equatorial isomer is too shallow for this structure to exist for even a very short time at 300 K. The pseudorotation must occur as part of the overall dissociation reaction rather than as a separate step.

3.3. The Reaction at 0 K in DMSO. In this section, the effects on the Wittig reaction of the introduction of a solvent will be considered. Finite temperature effects are not included at this stage. Calculations where both the solvent and finite temperature are included will be discussed in the next section.

The potential energy curves calculated for the two steps of the Wittig reaction are shown in Figure 5. The reaction energies and barriers extracted from these curves are listed in Table 3 along with the usual geometric parameters. The transition state and intermediate geometries are illustrated in Figure 4.

The potential energy curve with solvation behaves very differently from the gas-phase curve. Both curves show a very low maximum at about $R_1 = 4.0$ Å. In the gas-phase calculations this maximum precedes the van der Waals complex and a slightly higher maximum, which is taken as the transition state of the addition reaction, and the potential energy curve then drops about 20 kcal/mol to a minimum corresponding to the oxaphosphetane intermediate (see Figure 2). In contrast, when solvent effects are included the internal energy curve decreases from $R_1 = 4.0$ Å and has two minima between $R_1 = 2$ and 3 Å. The maximum at $R_1 = 4.0$ Å is taken as the transition state of the addition reaction (TS 1). The structure at this value of R_1 is illustrated in Figure 4a. In both of the minima (Int 1 and Int 2) the values of R_{CC}, R_{PC}, and R_{CO} in Table 2 are roughly in line

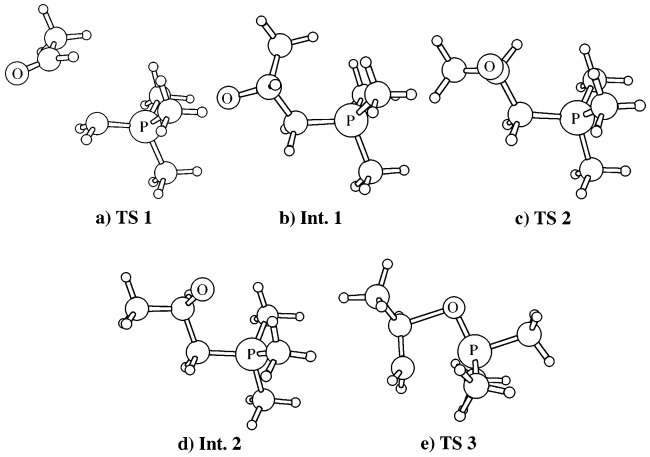

Figure 4. Structures of the transitions states and intermediates of the Wittig reaction in DMSO at 0 K. All unlabeled atoms are either C or H.

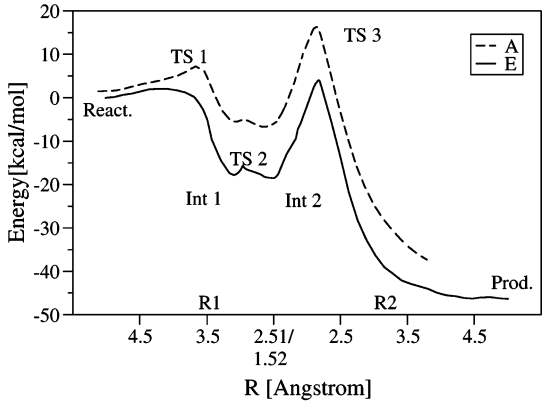

Figure 5. Helmholtz free energy and potential energy as a function of reaction coordinate of the Wittig reaction in DMSO.

TABLE 3: Energy Changes and Geometrical Parameters of the Wittig Reaction in DMSO at 0 K[a]

	ΔE	R_{1or2}	R_{PC}	R_{CO}	R_{CC}	R_{PO}	ϕ_{PCCO}
reactants	0.0		1.72	1.23			
TS 1	2.9	4.00	1.72	1.24	2.90	5.00	−162
Int 1	−17.8	3.11	1.82	1.39	1.56	4.10	−176
TS 2	−15.7	2.98	1.83	1.38	1.64	3.75	−88
Int 2	−18.5	2.51/1.52	1.82	1.39	1.56	3.04	−53
TS 3	4.1	2.20	2.48	1.71	1.44	1.62	−2
products	−46.3				1.34	1.53	

[a] Energies in kcal/mol. Distances in Å. Angles in degrees.

with what would be expected for a single bond. R_{PO} is very large for both intermediates at about 4 Å in the first minimum and 3 Å in the second. The structures corresponding to the two intermediates are illustrated in Figure 4b,d. The second minimum is slightly lower in energy than the first.

The calculations clearly predict that in DMSO the intermediate in the Wittig reaction of $CH_2P(CH_3)_3$ with CH_4CHO will have a betaine rather than an oxaphosphetane structure.

The two minima correspond to different relative orientations of the C−O and C−P bonds. In the first minimum (Int 1) they are anti with a PCCO dihedral angle of −176° while in the second minimum (Int 2) they are gauche with a dihedral angle of −53°. A similar minimum was found at about +50°. It was slightly higher in energy and was not pursued in detail. It is a little surprising that the anti conformation is higher in energy than the gauche conformation since the former would be expected to have a greater dipole moment and therefore interact more strongly with the solvent. The gauche conformer is probably stabilized by the electrostatic interaction between the partial charges on the P and O atoms. The barrier between the two intermediate structures is 2.8 kcal/mol relative to the second minimum. This may be an underestimate as the reaction coordinate is not ideal for describing the transformation between the two structures.

No minimum corresponding to the oxaphosphetane was found once solvent effects were introduced. One very shallow minimum corresponding to a structure very similar to the oxaphosphetane was found. This structure had similar values of R_{CC}, R_{CO}, and R_{PC} to the oxaphosphetane structure obtained in the vacuum and a ϕ_{PCCO} of −6° but a somewhat elongated value of R_{PO} of 2.07 Å. It is found at a value of the reaction coordinate R_1 of 1.92 Å. This minimum is not shown in Figure 5 as it is beyond the region where the betaine structures are found and is not on the lowest energy path from reactants to products. It is 14.6 kcal/mol below the reactants, which can be compared with the energy of the oxaphosphetane relative to reactants of −18.1 kcal/mol. Thus, the oxaphosphetane is destabilized a little by solvation but the betaine is stabilized significantly and is the preferred intermediate.

It should be kept in mind that the solvent chosen for the present study (DMSO) is one of the more polar used with the Wittig reaction. Less polar solvents such as THF or toluene would be expected to stabilize the betaine structures less relative to reactants. This suggests a qualitative model where the expected structure of the most stable intermediate of the Wittig reaction in a given solvent could be predicted by simply taking an appropriate property of the solvent (for example, the dielectric constant) as an indicator of where the betaine structures are relative to the oxaphosphetane and reactants which are approximately fixed in energy. Calculations of the potential energy curve of the present reaction in the presence of a few more solvents would be required to properly calibrate such a model.

The potential energy curve of the dissociation reaction in the presence of a solvent is also illustrated in Figure 5. The qualitative shape of the part of the internal energy curve corresponding to the dissociation of the betaine from the second intermediate is similar to that of the reaction in a vacuum. Obviously, the structure of the intermediate is different. A four-membered-ring oxaphosphetane structure is passed through about halfway to the transition state at $R_2 = 1.84$ Å. The oxygen atom is axial at this stage and the molecule undergoes a pseudorotation before reaching the transition state, which again has the oxygen equatorial. The minimum energy of the O-equatorial structure is somewhat higher in energy when solvation is included and is over 4 kcal/mol above the O-axial minimum (Int 2).

The structure of the transition state of the dissociation reaction is almost unchanged from that of the same reaction in the vacuum (compare Figures 1c and 4e). The value of R_2 is almost identical and the other geometric parameters are also very similar. In terms of energy, this transition state is slightly destabilized relative to the reactants, the intermediate, and the association transition state in comparison with the gas-phase calculations.

The overall reaction energy is calculated to be −46.3 kcal/mol, which is slightly more exothermic than the gas-phase value of −44.4 kcal/mol.

3.4. The Reaction at 300 K in DMSO. The final set of calculations to be discussed include both solvent and finite temperature effects. The results of these calculations are summarized in Table 4 and in Figure 5.

TABLE 4: Free Energy Changes and Geometrical Parameters of the Wittig Reaction in DMSO[a]

	ΔA	R_{1or2}	R_{PC}	R_{CO}	R_{CC}	R_{PO}	ϕ_{PCCO}
reactants	0.0						
TS 1	6.7	3.64	1.72	1.26	3.56	3.71	7
Int 1	−6.6	3.09	1.82	1.39	1.59	4.03	−176
TS 2	−6.2	2.98	1.83	1.39	1.61	3.81	−107
Int 2	−7.8	2.68/1.43	1.82	1.39	1.57	3.24	−57
TS 3	17.0	2.18	2.45	1.77	1.44	1.62	−3
products	−44.3[b]						

[a] Energies in kcal/mol. Distances in Å. Angles in degrees. [b] Estimated value.

Unfortunately, the discussion in the present section can only be qualitative because of difficulties encountered in obtaining long enough trajectories at all points along the reaction coordinate. In the reactants and products regions of the reaction the calculations including solvation were very unstable and tended to fail after a period of time. We are as yet unsure as to what the cause of the instability in the solvated might be. It becomes apparent over only a few time steps and causes the calculation to fail in only a few more. This instability does not suggest that the results obtained for stable simulations are incorrect. A previous study[27] has shown that the implementation of COSMO employed here shows correct energy conservation properties and gives reasonable results.

The zero-temperature calculations described in the previous section were short enough that any problems with stability could be avoided. Unfortunately, this was not the case in the 300 K simulations and it was virtually impossible to obtain the full 3.6 ps trajectories at values of R_1 or R_2 greater than 3.7 Å. In most of the large R_1 cases trajectories of about 1.0 ps or more could be derived before the calculations failed. The second half of each of the trajectories obtained before instability set in was used to evaluate $\langle F \rangle$. These ensemble average forces are less reliable than those discussed previously and for values of R_1 less than 3.7 Å the values of ΔA obtained from them will be less accurate. No simulations of appreciable length could be performed for values of R_2 greater than 3.7 Å.

Nevertheless, the free energy profile obtained in the presence of the solvent (Figure 5) combines features of the gas-phase free energy profile and the solvated potential energy curve. The initial addition reaction has a significant barrier corresponding to the loss of rotational entropy of the reactants. Two minima corresponding to betaine intermediates are found with the gauche structure lower in energy. A considerable barrier to the elimination reaction is found.

The maximum in the free energy curve corresponding to the addition reaction is interesting in that, as was the case of the gas-phase reaction, the increase in free energy is mostly due to the loss of rotational entropy of the reactant molecules but in contrast to the gas-phase case the new bond is forming as the rotational entropy is being lost. In the gas-phase calculations the maxima in the potential energy curve and free energy profile of the addition reaction occur at similar values of the reaction coordinate. The height of the free energy barrier at 12.7 kcal/mol is comparable to the total rotational entropy of the two reactant molecules multiplied by T, which is about 15 kcal/mol. In the solvated case, the maxima in the free energy profile and potential energy curve occur at rather different values of the reaction coordinate ($R_1 = 3.6$ and 4.0 Å, respectively). When $R_1 = 3.6$ Å the potential energy is slightly negative (−1 kcal/mol) and decreasing fairly rapidly as R_1 decreases. In this part of the reaction the C−C bond is forming, leading to a decrease in the potential and free energy of the system, but the reactants are losing rotational entropy leading to an increase in the free energy. Up until $R_1 = 3.6$ Å the contribution to the free energy from the loss of rotational entropy wins out and the free energy increases. After $R_1 = 3.6$ Å the contribution from the C−C bonds is greater and the free energy begins to decrease. The free energy barrier to this reaction in solution is thus again due solely to entropy but this time is only about 7 kcal/mol in height, much less than the rotational entropy of the reactants, because it is partially canceled by the increasing bonding interaction between the two carbon atoms. That the reactant molecules still have significant rotational entropy at this stage is reinforced by the average value of ϕ_{PCCO} at $R_1 = 3.6$ Å. At 7° it is completely different from the value of −162 ° obtained at 0 K. The average dihedral angle at 300 K is so different because the molecule rotates quite easily about the CC axis giving an average angle close to zero.

The free energies of reaction to form the intermediates are about 10 kcal/mol higher than the equivalent changes in potential energy just as was the case in the gas-phase calculations. The average structures of the intermediates are much the same as the structures corresponding to the minima in the potential energy curve. These calculations therefore suggest that at 300 K the intermediates in this Wittig reaction will have a betaine structure. The value of R_1 at which the second minimum in the free energy curve appears is slightly larger than that of the potential energy curve.

The free energy barrier between the gauche and anti isomers of the betaine is even lower than the potential energy barrier. The barrier is less than 2 kcal/mol and rotation about the C−C bond should occur fairly rapidly. Such rotation was not observed in the present simulations as it was hindered by the constraint describing the reaction coordinate.

The dissociation reaction free energy profile has a very similar shape to the potential energy curve of this part of the reaction. The average structure at the transition state is also very similar to the structure corresponding to the maximum in the potential energy curve. It occurs at a value of R_2 much like that found in the previous calculations. It appears that this step in the reaction occurs in a very similar manner no matter whether it is in the gas phase or solvated or whether finite temperature effects are allowed for or not.

The total free energy change of the reaction in DMSO cannot be calculated because simulations could not be carried out for values of R_2 greater than 3.83 Å. Given that this part of the reaction appears to be very similar in all of the calculations discussed here, a reasonable estimate for ΔA_{tot}(DMSO) can be derived by using the gas-phase free energy profile. The gas-phase calculations give a change in free energy of about 7.2 kcal/mol from $R_2 = 3.8$ Å to products. If this estimate is added to the value of ΔA(DMSO) at $R_2 = 3.8$ Å of −37.1 kcal/mol an approximate value of −44.3 kcal/mol is obtained for the total reaction free energy. This result is similar to that obtained in all of the previous calculations and suggests that solvation and entropy effects have little influence on the overall reaction energy of Wittig reactions.

4. Conclusion

It has long been known that entropic contributions to the free energies of addition and elimination reactions should be large and that introducing solvation can have a significant effect on any reaction where charge separation or ionization can occur. The calculations described here show that this certainly is the case for the Wittig reaction. Calculations including finite temperature and solvent effects give a very different picture of

how this reaction proceeds when compared to what is obtained from conventional gas-phase calculations at 0 K.

When finite temperature or entropy effects are included, the initial addition reaction is no longer approximately barrierless but has a significant barrier of about 10 kcal/mol caused by the requirement that the two reacting molecules cease rotating with respect to each other. The free energy of this reaction is less negative than its potential energy change and the final dissociation step has a more negative free energy change than potential energy change. Shallow minima on the 0 K reaction curve, such as the van der Waals complex of the reactants, are found to have negligible influence once the system is heated to 300 K. The overall reaction conserves the number of molecules and as a result, entropy effects have a minimal effect on the total reaction energy.

Solvation has little effect on the early and late parts of the reaction, but it strongly influences the middle part of the reaction. A different intermediate is obtained from that predicted by gas-phase calculations. Two possible intermediates have generally been accepted in the literature. Previous calculations have always suggested that only the relatively nonpolar oxaphosphetane intermediate participates in the reaction. No sign of a minimum in the potential energy surface corresponding to the dipolar betaine intermediate has been found. The present work suggests that when the reaction is carried out in a fairly polar solvent such as DMSO the betaine intermediate will in fact be present.

Overall, these results suggest that calculations modeling systems at 0 K in the gas phase can often be deceptive when attempting to gain insight into reactions performed in solution at significant temperatures. Entropy corrections to energy differences between two minima on a potential energy surface are relatively straightforward to calculate with formulas available in many text books.[29] The effects on other values of the reaction coordinate such as transition states are less easily predicted a priori. For example, the first step in the Wittig reaction in the gas phase was found here to have a significant barrier in its free energy curve when only a very small barrier was found on the potential energy curve. In a previous study, the acid−base reaction of BH_3 and NH_3 was found to proceed with little to no barrier in both the internal and free energy curves.[39] The first step of the Wittig reaction in DMSO is intermediate between these two extremes. Thus, an addition reaction that has little to no barrier in its potential energy curve may have an identical barrier, a slightly higher barrier, or a much higher barrier in its free energy profile depending on the specifics of the reaction.

Solvation clearly must be considered if there is a chance that charge separation can occur either through the formation of ions or a dipolar structure as was the case here. If ions are present from the beginning then some treatment of solvation is of course crucial if there is any hope of modeling a reaction carried out in a solvent in a reasonable way.

Acknowledgment. We would like to acknowledge the use of the Westgrid computational resources in carrying out some of the calculations described here. T. Z. would like to thank the Canadian government for a Canada research chair in theoretical inorganic chemistry. M.S. would like to thank Wendy Lines for helpful discussions.

References and Notes

(1) Wittig, G.; Schöllkopf, U. *Chem. Ber.* **1954**, *87*, 1318−1330.
(2) Wittig, G. *Pure Appl. Chem.* **1964**, *9*, 245−254.
(3) Vedejs, E.; Peterson, M. J. *Top. Stereochem.* **1994**, *21*, 1−157.
(4) Maryanoff, B.; Reitz, A. *Chem. Rev.* **1989**, *89*, 863−927.
(5) Vedejs, E.; Meier, G. P.; Snoble, K. A. J. *J. Am. Chem. Soc.* **1981**, *103*, 2823−2831.
(6) Vedejs, E.; Marth, C. F. *J. Am. Chem. Soc.* **1989**, *111*, 1519−1520.
(7) Vedejs, E.; Marth, C. F. *J. Am. Chem. Soc.* **1990**, *112*, 3905−3909.
(8) Reitz, A. B.; Mutter, M. S.; Maryanoff, B. E. *J. Am. Chem. Soc.* **1984**, *106*, 1873−1875.
(9) Lopez-Ortiz, F.; Lopez, J. G.; Manzaneda, R. A.; Alvarez, I. J. P. *Mini-Rev. Org. Chem.* **2004**, *1*, 65−76.
(10) Höller, R.; Lischka, H. *J. Am. Chem. Soc.* **1980**, *102*, 4632−4635.
(11) Volatron, F.; Eisenstein, O. *J. Am. Chem. Soc.* **1984**, *106*, 6117−6119.
(12) Volatron, F.; Eisenstein, O. *J. Am. Chem. Soc.* **1987**, *109*, 1−14.
(13) Naito, T.; Nagase, S.; Yamataka, H. *J. Am. Chem. Soc.* **1994**, *116*, 10080−10088.
(14) Mari, F.; Lahti, P. M.; McEwen, W. E. *Heteroatom. Chem.* **1990**, *1*, 255.
(15) Mari, F.; Lahti, P. M.; McEwen, W. E. *Heteroatom. Chem.* **1991**, *2*, 265.
(16) Mari, F.; Lahti, P. M.; McEwen, W. E. *J. Am. Chem. Soc.* **1992**, *114*, 813−821.
(17) Yamataka, H.; Nagase, S. *J. Am. Chem. Soc.* **1998**, *120*, 7530−7536.
(18) Lu, W. C.; Wong, N.; Zhang, R. Q. *Theor. Chem. Acc.* **2002**, *107*, 206−210.
(19) Tomasi, J.; Persico, M. *Chem. Rev.* **1994**, *94*, 2027−2094.
(20) Cramer, C. J.; Truhlar, D. G. In *Quantitative Treatments of Solute/Solvent Interactions*; Politzer, S., Murray, J. S., Eds.; Elsevier: Amsterdam, The Netherlands, 1994; pp 9−54.
(21) Cramer, C. J.; Truhlar, D. G. In *Reviews in Computational Chemistry*; Lipkowitz, K. B., Boyd, D. B., Eds.; VCH: New York, 1995; Vol. 6, pp 1−72.
(22) Rivail, J.; Rinaldi, D. In *Computational Chemistry, Reviews of Current Trends*; Leszcynski, J., Ed.; World Scientific: New York, 1995; Vol. 1, pp 139−174.
(23) Tomasi, J.; Mennucci, B. In *Encyclopedia of Computational Chemistry*; Schleyer, P., Ed.; Wiley: Chichester, UK, 1998; Vol. 4, pp 2547−2560.
(24) Cramer, C. J.; Truhlar, D. G. *Chem. Rev.* **1999**, *99*, 2161−2200.
(25) Klamt, A.; Schüürmann, G. *J. Chem. Soc., Perkin Trans. 2* **1993**, 799.
(26) Klamt, A. In *Encyclopedia of Computational Chemistry*; Schleyer, P. v. R., Ed.; Wiley: Chichester, UK, 1998; Vol. 1, pp 604−615.
(27) Senn, H. M.; Margl, P. M.; Schmid, R.; Ziegler, T.; Blöchl, P. *J. Chem. Phys.* **2003**, *118*, 1089−1100.
(28) Straatsma, T. P. In *Reviews in Computational Chemistry*; Lipkowitz, K. B., Boyd, D. B., Eds.; VCH: New York, 1996; Vol. 9, pp 81−127.
(29) McQuarrie, D. A. *Statistical Thermodynamics*; Harper and Row: New York, 1973.
(30) Becke, A. D. *Phys. Rev. A* **1988**, *38*, 3098−3100.
(31) Perdew, J. P. *Phys. Rev. B* **1986**, *33*, 8822−8824.
(32) Perdew, J. P.; Wang, Y. *Phys. Rev. B* **1992**, *45*, 13244−13249.
(33) Car, R.; Parrinello, M. *Phys. Rev. Lett.* **1985**, *55*, 2471−2474.
(34) Blöchl, P. E. *Phys. Rev. B* **1994**, *50*, 17953−17979.
(35) Marx, D.; Hutter, J. In *Modern Methods and Algorithms of Quantum Chemistry*; Grotendorst, J., Ed.; John von Neuman Institute of Computing: Jülich, 2000; Vol. 1 of *NIC*, pp 301−449.
(36) Andersen, H. C. *J. Chem. Phys.* **1980**, *72*, 2384−2393.
(37) Blöchl, P. E. *J. Chem. Phys.* **1995**, *103*, 7422−7428.
(38) Blöchl, P. E.; Först, C. J.; Schimpl, J. *Bull. Mater. Sci.* **2003**, *26*, 33−41.
(39) Kelly, E.; Seth, M.; Ziegler, T. *J. Phys. Chem. A* **2004**, *108*, 2167−2180.